Construction and Building Materials 138 (2017) 45–55

Contents lists available at ScienceDirect

Construction and Building Materials

journal homepage: www.elsevier.com/locate/conbuildmat

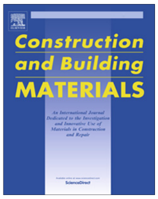

Localization of cracks in cementitious materials under uniaxial tension with electrical resistance tomography

Xiaoyong Zhou [a,*], Prakash Bhat [b], Hui Ouyang [a], Jiagan Yu [a]

[a] *Faculty of Engineering, China University of Geosciences, Wuhan, Hubei 430074, China*
[b] *Siemens PLM Software Inc., Houston, TX 77042, USA*

HIGHLIGHTS

- Study on cracks detection of ECC under uniaxial tension with ERT.
- The ERT system is assembled with an AC source, a voltage acquisition instrument, and an ESM.
- For the rectangular ECC test specimen, BEEA yields better results than UPEA using ERT.

ARTICLE INFO

Article history:
Received 13 April 2016
Received in revised form 28 January 2017
Accepted 29 January 2017

Keywords:
Electrical resistance tomography
Engineered cementitious composite
Crack localization
Imaging reconstruction
Monotonic uniaxial tension
Non-destructive testing

ABSTRACT

This paper explores the feasibility of using electrical resistance tomography (ERT) for detecting damages or cracks on the engineered cementitious composites (ECC) under monotonic uniaxial tension loading. Two types of electrode arrays, unilateral planar electrodes array (UPEA) and bilateral edge electrodes array (BEEA) were developed and equipped in ERT system for ECC specimens and an electrode switching module (EMS) was designed to enforce the adjacent driver pattern of sixteen electrodes attached to the surface of ECC specimens. A constant and low frequency electric current (1 μa, 1.5 kHz) is applied onto the ECC specimen via some electrode pairs, and AC voltages were measured synchronously using the rest of electrode pairs. All these data were input into the inverse program to analyze and obtain the internal resistance distribution in the studied specimens. The capabilities of difference ERT to locate the cracks in ECC was estimated using (1) finite element models with given single crack and multiple cracks for image reconstruction, and (2) image reconstruction of real cracks in ECC plates under uniaxial tensile loading. The results showed that difference ERT could be used to detect the position and approximate range of the cracks produced in ECC and the performance of BEEA was better than that of UPEA.

1. Introduction

Concrete is one of the most versatile, safe, reliable and sturdy construction materials characterized with high compressive strength and low tensile strength. Compared with other building materials such as steel, wood, and resinous polymer, concrete is a brittle material. Although its low tensile strength can be compensated after reinforcement, its proneness to fracture is its proneness to fracture is unavoidable. When the tensile stress When the tensile stress applied on concrete due to external load, moisture, chemical, and thermal effect exceeds its tensile capacity [1–3], fractures will occur and propagate, resulting in a continuous degradation of its load-bearing capacity over time.

In order to understand cracks generation and propagation and rapidly, easily and effectively evaluate concrete structure, several non-destructive testing (NDT) techniques have been developed and widely used, such as acoustic emission and ultrasonic techniques [4–5], impact echo [6], ground-penetrating radar [7], and infrared thermography [8] as well as recently developed AC resistance measurements for concrete humidity [9,10] and chloride distributions [11,12]. Electrical resistance tomography (ERT) has been used to nondestructively monitor concrete structures [13], evaluate temporal evolution of moisture distribution in concrete [14], and monitor cracks in fiber reinforced cementitious composites during tensile loading [15]. Afterward, the ERT has expanded its applications to 3-D imaging of concrete samples in cylindrical geometries [16] to detect cracks in concrete [17], observe the distribution of moisture content in concrete specimens, and explore moisture movement along with the position and the approximate shape of water wave in cementitious composites [18]. [19]. The

---

* Corresponding author.
E-mail address: xyz@cug.edu.cn (X. Zhou).

http://dx.doi.org/10.1016/j.conbuildmat.2017.01.128
0950-0618/

development of a new electrical sensing skin opens a new way for utilizing with ERT for qualitative and quantitative detections as well as 2-D and 3-D imaging of damage and cracks in concrete [19–21]. Even ERT has been widely used to nondestructively detect defects in concrete, few studies utilized ERT to real-time monitor cracks in concrete under direct tensile and examined its efficiency and effectiveness. In this study, we investigated the capability of ERT for real-time detection of cracks in concrete subject to monotonic unilateral tension and simultaneous image reconstruction through data acquisition and processing. A 16 electrodes data acquisition system with an electrode switching module (ESM) was assembled firstly for high-speed, real-time data collection and two new designed electrode arrays, unilateral planar electrodes array (UPEA), and bilateral edge electrodes array (BEEA) were successively equipped on the surface of ECC specimens in tensile tests. Difference imaging scheme was used to analyze both modeled (error free) and measured (with errors) voltages. The results illustrated that the developed ERT system can be used for effective and real-time crack detection in cementitious materials.

2. Brief background on ERT

In the ERT for crack detection, the spatial distribution of electrical conductivity (σ) or resistivity (ρ) within a closed domain (Ω) is reconstructed by an image reconstruction algorithm from the surface potential produced by applying a constant electrical current the electrode pairs on the boundaries of the domain (Γ). The load-induced cracks are the physical inhomogeneity of ECC that interrupts or resists the local electric current flow and changes the distribution of local resistivity. Thus, the resultant map of resistance reflects the locations of cracks in the ECC. The reconstruction in ERT is an ill-posed inverse problem because its solution is not unique and depends on measurement and modeling [19,23]. The reconstruction in ERT is also an inverse problem, which means the solution of the forward problem is the basis of the inverse problem. And the forward model is used to calculate the electrode potentials in accordance with the given conditions, such as the internal electrical conductivity (σ) or resistivity (ρ) distribution, contact resistance, and the constant electrical current. When taking the contact resistance into account, the best mathematical model is the complete electrode model (CEM) [16,21,22], consisting of a Maxwell equation and its three boundary conditions.

$$\Omega : \nabla \cdot (\sigma \nabla \mu) = 0 \tag{1}$$

$$\Gamma_1 : \sigma \frac{\partial \varphi}{\partial \bar{n}} = 0 \tag{2}$$

$$\Gamma_2 : \int \sigma \frac{\partial \varphi}{\partial \bar{n}} dS = -I_l \tag{3}$$

$$\Gamma_3 : \varphi + z_l \sigma \frac{\partial \varphi}{\partial \bar{n}} = \phi_l \tag{4}$$

where Ω is a closed domain, Γ_1 is the exterior boundary without electrodes, Γ_2 is the exterior boundary with electrodes to apply an electric current, and Γ_3 is the exterior boundary with electrodes used for measuring potential, σ is the conductivity, φ is the potential in the closed domain Ω; I_l and ϕ_l are the current and potential through the l-th electrode, respectively; z_l is the contact resistance between the exterior boundary and the l -th electrode; $\bar{n}$ is outward unit normal; dS represents the differential cross area of one electrode, and $\sigma \frac{\partial \varphi}{\partial \bar{n}}$ is the current density. Further, Eq. (2) clearly indicates that no current flows in and out of the boundary Γ_1 without electrodes; Eq. (3) reveals that the surface integral of current density over the boundary Γ_2 is equal to the injected current [16,23]. Based on the principle of conservation of charges, the total input currents are equal to the total output currents in all of the boundary electrodes. The summation of potential at all boundary electrodes is equal to zero. Thus, Eq. (3) and Eq. (4) turn into the following corresponding forms [24]

$$\Gamma_2 : \sum_{l=1}^{L} I_l = 0 \tag{5}$$

$$\Gamma_3 : \sum_{l=1}^{L} U_l = 0 \tag{6}$$

where Γ_2 and Γ_3 are the boundary conditions, and L is the number of electrodes. It is difficult to find the analytic solution of such a boundary value with the complex geometry or boundary conditions. Thus, we have to appeal to the finite element method (FEM) to find an approximate solution. The observation model can be written as

$$V = R(\sigma, Z; I) + e \tag{7}$$

where V is the difference of potentials between selected electrodes, e is observation noise, and Z is the column vector consisting of contact resistances $z_l (l = 1,2,\ldots L)$. Note that, all the parameters in Eq. (7) are vectors. The function $R(\sigma, Z; I)$ appears in its matrix form and maps the relationship between electrode currents I and voltages V.

In difference imaging schemes, at least two sets of voltage data need to be measured for the inverse problem. One set of voltage data are collected on the uniform state usually before damages or cracks occur in the concrete and the other set of voltage data are collected on the perturbed state usually as damages or cracks develop. The changes in electrical conductivity can be calculated by using a dynamic imaging algorithm based on both sets of voltages data. As a result, a difference image can be reconstructed. According to the relationship between boundary voltages and interior conductivity, the solution to the problem can be obtained by the global linearization approach, i.e. Taylor expansion at σ_1 as follows:

$$V(\sigma_2) - V(\sigma_1) = V'(\sigma_1)[\sigma_2 - \sigma_1] + O(\sigma_2 - \sigma_1)^2 \tag{8}$$

According to Eq. (7), and ignoring the higher-order components $O(\sigma_2 - \sigma_1)^2$, Eq. (8) can be written as

$$\Delta V \approx \boldsymbol{J} \Delta\sigma + \Delta e \tag{9}$$

where σ_1 and σ_2 represent the initial conductivity and crack-induced conductivity, respectively; $\Delta V = V(\sigma_2) - V(\sigma_1)$, representing the difference in potentials measured from cracking state and initial state; $\Delta\sigma = \sigma_2 - \sigma_1$, representing the change in spatial conductivity used for imaging the distribution of cracks; $\Delta e = e(\sigma_2) - e(\sigma_1)$, representing the difference in observation noises between these two states; and $J = V'(\sigma_1)$ so-called the Jacobian mattrix. In difference imaging scheme, the observation noise decreases largely significantly after subtraction. Consequently, measurements with relative low-precision can achieve the satisfactory results in the reconstruction map. This is the main reason why the difference imaging scheme other than absolute imaging scheme is chosen in this study. Cheney et al. has solved Eq. (9) using their NOSER algorithm [25]. In this study, the NOSER was used to solve the ill-posed inverse problem. This algorithm is based on the method of least squares. It takes only one step of a Newton's method, using a constant conductivity as an initial guess. Most of the calculations can be done analytically. NOSER is performed by assuming a smooth and uniform conductivity distribution at the reference state (initial state). It does not reproduce the absolute change in the electrical conductivity accurately, unless the initial